Constructing CeO_{2-x}@CoFe-Layered Double Hydroxides heterostructure as an improved electrocatalyst for highly efficient water oxidation

Yiming Hu[a†], Wenjun Liu[a†], Kun Jiang[a], Li Xu[a], Meili Guan[a], Jian Bao[a*], Hongbing Ji[b*], Hua-ming Li[a]

a. Institute for Energy Research, School of Chemistry and Chemical Engineering, School of Material Science & Engineering, Jiangsu University, Zhenjiang, Jiangsu, 212013, P. R. China.

b. Fine Chemical Industry Research Institute, School of Chemistry, Sun Yat-sen University, Guangzhou 510275, P.R.China

†These authors contributed equally to this work.

***Corresponding Authors**

Email: baojian@ujs.edu.cn

Email: jihb@mail.sysu.edu.cn

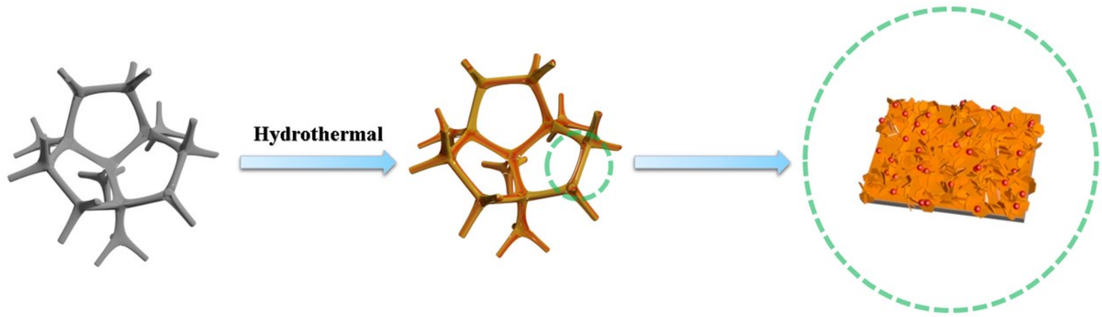

Scheme S1. Scheme image of synthesis of CeO_{2-x}@CoFe LDH/NF by a facile hydrothermal method.

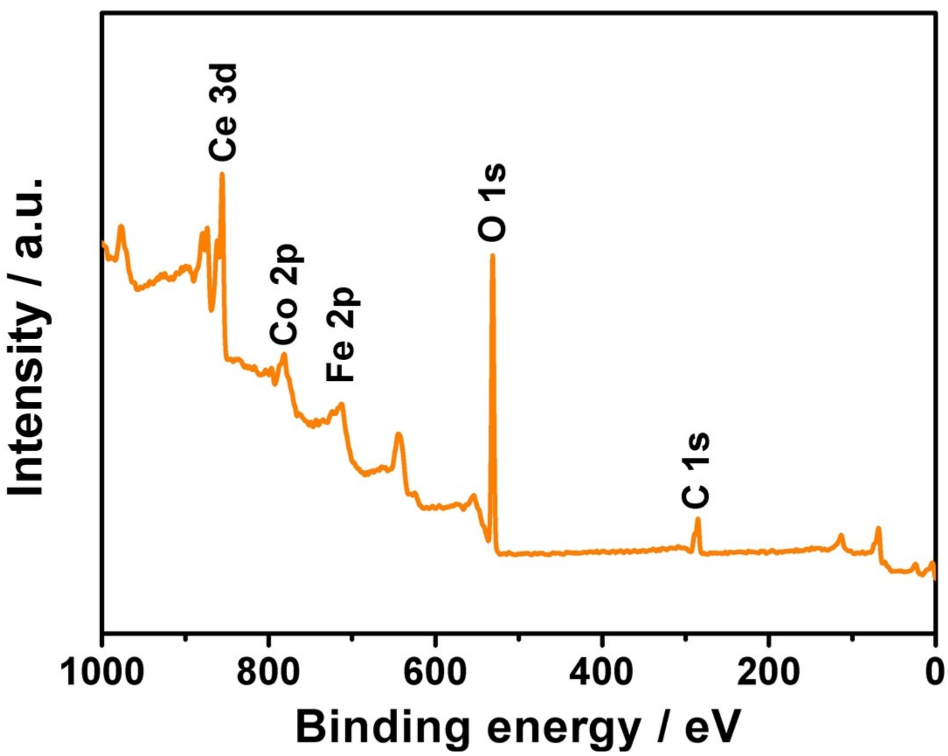

Figure S1. XPS survey spectrum of CeO_{2-x}@CoFe LDH/NF.

Figure S1 is the XPS survey spectrum of CeO_{2-x}@CoFe LDH/NF which shows the Co, Fe, Ce and O elements in the obtained material.

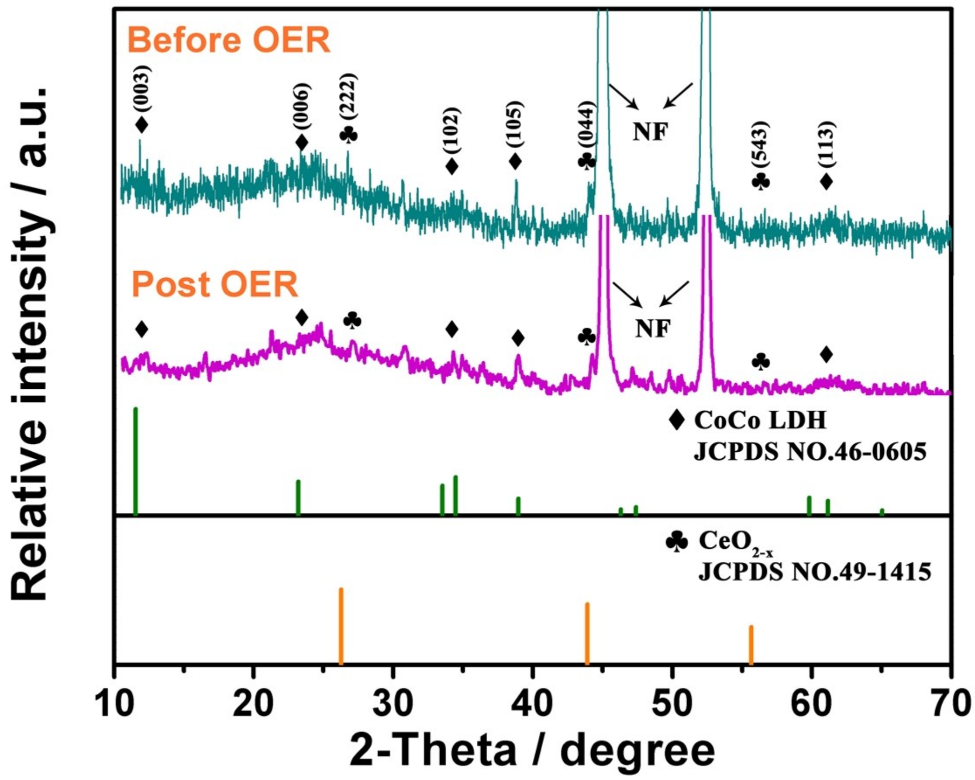

Figure S2. XRD patterns of CeO_{2-x}@CoFe LDH/NF before and after OER.

As shown in Figure S2, the crystal phase of CeO_{2-x}@CoFe LDH/NF has not changed significantly after the OER test, which indicates the good stability of the material.

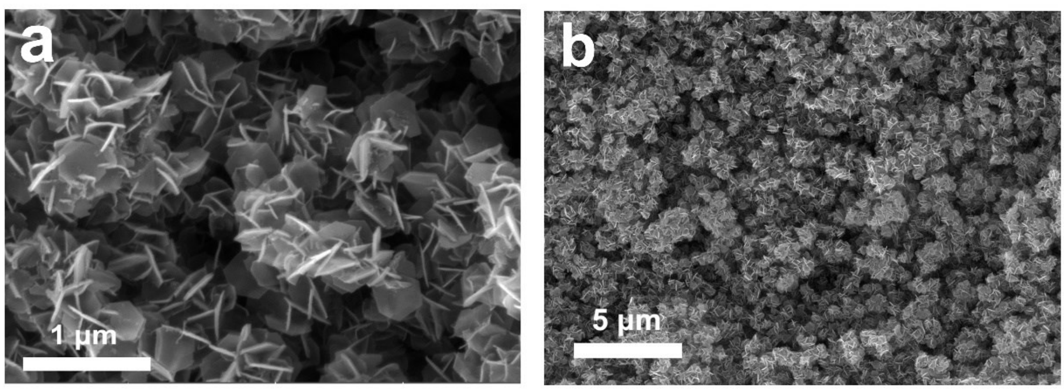

Figure S3. (a, b) SEM images of CeO_{2-x}@CoFe LDH/NF with different magnifications.

As shown in Figure S3, the SEM images at different magnifications further clarify that the morphology of the main material is nanosheet array structure.

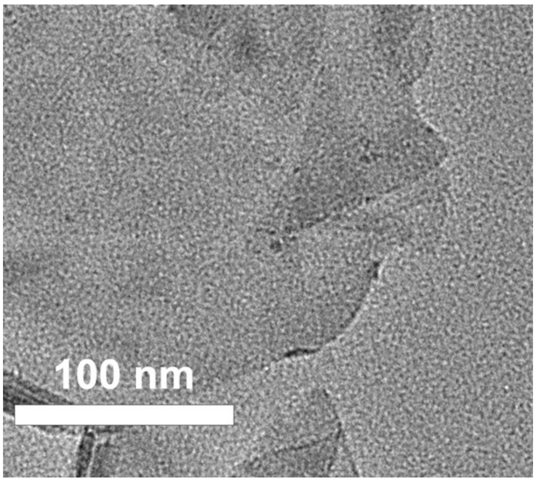

Figure S4. TEM image of CoFe LDH.

The TEM image of CoFe LDH is shown in Figure S4, which indicates its nanosheet structure.

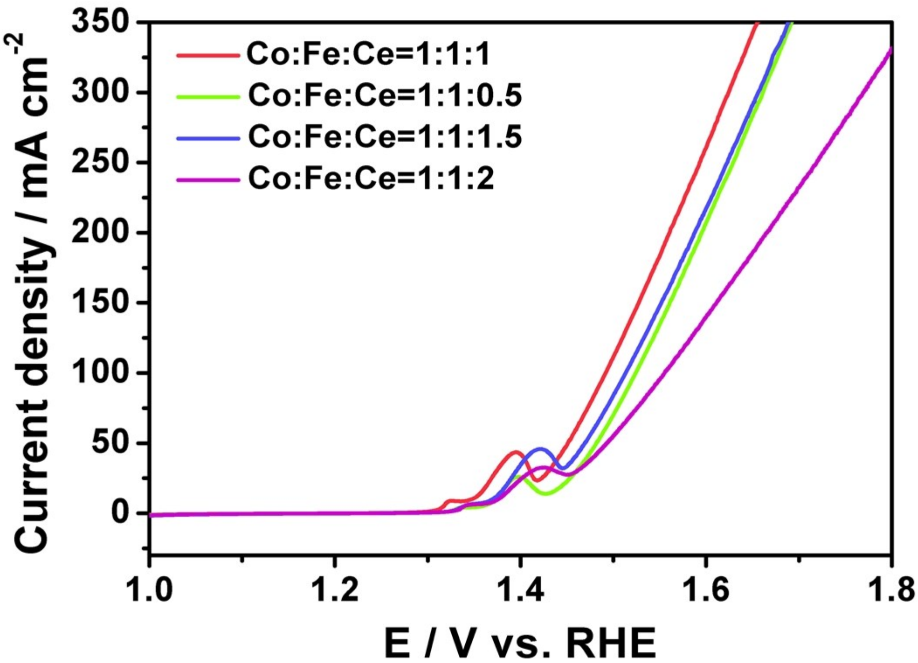

Figure S5. Polarization curves of samples with different amount of Ce in OER.

As shown in Figure S5, the sample with the metal ratio (Co: Fe: Ce) of 1:1:1 shows the best OER performance, which is also the main catalyst in this work, defined as CeO_{2-x}@CoFe LDH/NF.

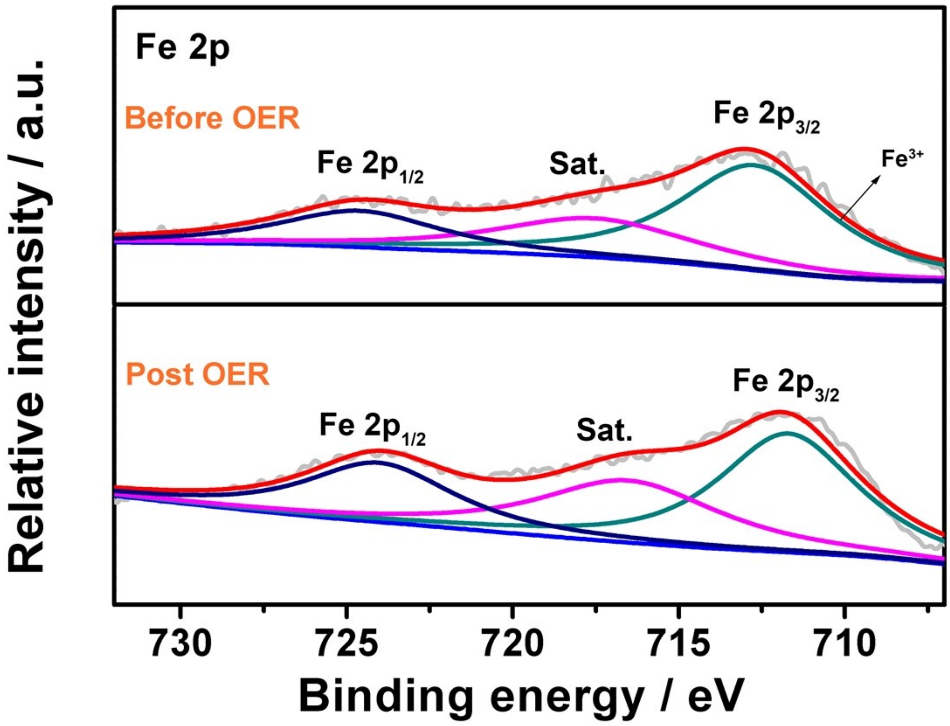

Figure S6. XPS spectrum of Fe 2p for CeO_{2-x}@CoFe LDH/NF before and after OER.

As shown in Figure S6, the Fe 2p for CeO_{2-x}@CoFe LDH/NF indicates Fe^{3+} in the obtained material before and after OER.

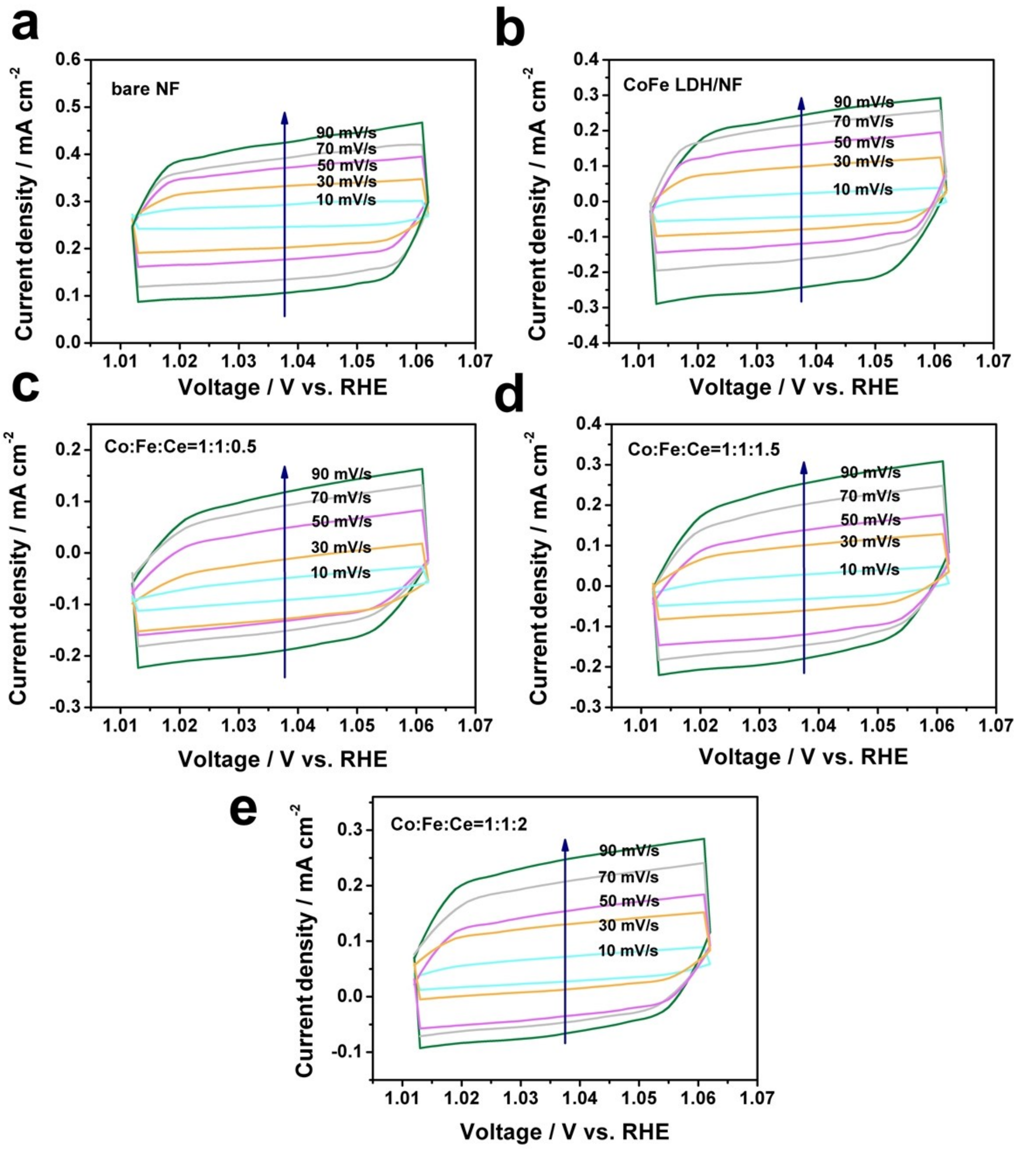

Figure S7. (a-e) CV curves of a series of comparative samples at different scan rates from 10 to 90 mV/s.

Table S1. Summary of ICP results of CeO_{2-x}@CoFe LDH/NF.

Sample	Added value of Co, Fe, Ce (Molar ratio)	The calculated of Co, Fe, Ce (Atomic ratio)
CeO_{2-x}@CoFe LDH/NF	1: 1: 1	1: 0.6: 1.1

Table S2. Impedance fitting results of CeO_{2-x}@CoFe LDH/NF, CoFe LDH/NF and bare NF.

Sample	R_s (Ω)	R_{ct} (Ω)
CeO_{2-x}@CoFe LDH/NF	1.446	0.766
CoFe LDH/NF	1.440	1.098
bare NF	1.705	59.29

R_s value is used to describe the resistance of solution, R_{ct} represents the resistances of charge transfer; and C_{dl} value is the double-layer capacitance.

Table S3. Electrocatalysis results of as-prepared CeO_{2-x}@CoFe LDH/NF and some reported electrocatalysts.

Catalysts	Electrolyte	η at *j*=100 mA cm^{-2} (mV)	References
CeO_{2-x}@CoFe LDH/NF	1 M KOH	204	This work
NiV-LDH@FeOOH/NF	1 M KOH	297	1
$NiCo_2O_4$	1 M KOH	320	2
NiFe LDH/NF	1 M KOH	222	3
CoO/CoFe LDH	1 M KOH	292	4

partially amorphous-NiFeLDH /Nickel Iron Foam	1 M KOH	326	5
Iron doped nickel hydroxide/NF	1 M KOH	312	6
$CoSn_2$/Ni Foam	1 M KOH	360	7
Ni_3S_2@NiV-LDH	1 M KOH	320	8
(Co-Pi)	1 M KOH	420	9
Au-Ir	1 M KOH	245	10
$Co_2Mo_3O_8$	1 M KOH	241	11

References:

[1] W. Bao, L. Xiao, J. Zhang, Z. Deng, C. Yang, T. Ai, X. Wei, Interface engineering of NiV-LDH@FeOOH heterostructures as high-performance electrocatalysts for oxygen evolution reaction in alkaline conditions. *Chem. Commun.,* 2020, **56**, 9360-9363.

[2] J. Béjar, L. Álvarez-Contreras, J. Ledesma-García, N. Arjon, L. Arriaga, An advanced three-dimensionally ordered macroporous $NiCo_2O_4$ spinel as a bifunctional electrocatalyst for rechargeable Zn–air batteries. *J. Mater. Chem. A,* 2020, **8**, 8554-8565.

[3] H. Yang, C. Wang, Y. Zhang, Q. Wang, Green synthesis of NiFe LDH/Ni foam at room temperature for highly efficient electrocatalytic oxygen evolution reaction. *Sci. China. Mater.,* 2019, **62**, 681-689.

[4] Z. Gao, T. Ma, X. Chen, H. Liu, L. Cui, S. Qiao, J. Yang, Strongly Coupled CoO Nanoclusters / CoFe LDHs Hybrid as a Synergistic Catalyst for Electrochemical Water Oxidation, *Small,* 2018, **14**, 1800195–1800203.

[5] J. Xie, H. Qu, F. Lei, X. Peng, W. Liu, L. Gao, P. Hao, G. Cui, B. Tang, Partially amorphous nickel–iron layered double hydroxide nanosheet arrays for robust bifunctional electrocatalysis. *J. Mater. Chem. A,* 2018, **6**, 16121-16129.

[6] C. Guo, C. Li, Room temperature-formed iron-doped nickel hydroxide on nickel foam as a 3D electrode for low polarized and high-current-density oxygen evolution. *Chem. Commun.,* 2018, **54**, 3262-3265.

[7] P. Menezes, C. Panda, S. Garai, C. Walter, A. Guiet, M. Driess, Structurally Ordered Intermetallic Cobalt Stannide Nanocrystals for High-Performance Electrocatalytic Overall Water-Splitting. *Angew. Chem. Int. Ed.,* 2018, **57**, 15237-15242.

[8] Q. Liu, J. Huang, Y. Zhao, L. Cao, K. Li, N. Zhang, D. Yang, L. Feng, L. Feng, Tuning the coupling interface of ultrathin Ni_3S_2@NiV-LDH heterogeneous nanosheet electrocatalysts for improved overall water splitting. *Nanoscale,* 2019, **11**, 8855-8863.

[9] J. Qi, J. Xie, Z. Wei, S. Lou, P. Hao, F. Leia, B. Tang, Modulation of crystal water in cobalt phosphate for promoted water oxidation. *Chem. Commun.,* 2020, **56**, 4575-4578.

[10] R. Du, J. Wang, Y. Wang, R. Hübner, X. Fan, I. Senkovska, Y. Hu, S. Kaskel, A. Eychmüller, Unveiling reductant chemistry in fabricating noble metal aerogels for

superior oxygen evolution and ethanol oxidation. *Nat. Commun.,* 2020, **11**, 1590.
[11] Z. Liu, T. Ouyang, X. Wang, X. Mai, A. Chen, Z. Tang, Coupling Magnetic Single-Crystal $Co_2Mo_3O_8$ with Ultrathin Nitrogen-Rich Carbon Layer for Oxygen Evolution Reaction. *Angew. Chem. Int. Ed.,* 2020, **59**, 11948-11957.